PHYSICAL REVIEW B **69**, 180503(R) (2004)

Effect of morphology on the superconductor-insulator transition in one-dimensional nanowires

A. T. Bollinger, A. Rogachev, M. Remeika, and A. Bezryadin
Department of Physics, University of Illinois at Urbana-Champaign, Urbana, Illinois 61801-3080, USA
(Received 19 January 2004; published 5 May 2004)

We study the effect of morphology on the low-temperature behavior of superconducting nanowires which vary in length from 86 nm to 188 nm. A well-defined superconductor-insulator transition is observed only in the family of homogeneous wires, in which case the transition occurs when the normal resistance is close to $h/4e^2$. Inhomogeneous wires, on the other hand, exhibit a mixed behavior, such that signatures of the superconducting and insulating regimes can be observed in the same sample. The resistance versus temperature curves of inhomogeneous wires show multiple steps, each corresponding to a weak link constriction (WLC) present in the wire. Similarly, each WLC generates a differential resistance peak when the bias current reaches the critical current of the WLC. Due to the presence of WLC's an inhomogeneous wire splits into a sequence of weakly interacting segments where each segment can act as a superconductor or as an insulator. Thus the entire wire then shows a mixed behavior.

DOI: 10.1103/PhysRevB.69.180503 PACS number(s): 74.40.+k, 73.21.Hb, 74.78.Na

Evidence for a superconductor-insulator quantum phase transition (SIT) in one-dimensional (1D) wires has been found in a number of experiments.[1,2] Yet, other studies have demonstrated a crossover, as opposed to a SIT, in thin wires where superconductivity disappears gradually, as diameter is reduced, presumably due to an increasing number of quantum phase slips (QPS).[3–5] Thus the existence and possible origins of superconductor-insulator transitions in 1D remain important open problems. In particular, it is not known how the SIT depends on the morphology of nanowires.

In two-dimensional system, for example, the crucial role of morphology (i.e., granularity) on the SIT is well known.[6–8] For uniform films, as the film thickness is reduced, a reduction of the critical temperature is observed while the superconducting transition remains sharp. The SIT occurs when the square resistance of the film reaches a critical value close to the quantum resistance $R_Q = h/4e^2 = 6.5\ \mathrm{k}\Omega$.[9] In nonhomogeneous (granular) films, on the other hand, a reduction of the film thickness results in a *crossover* between superconducting and insulating regimes, with very broad resistive transitions in the thinnest superconducting samples.[6,10,11] Our goal here is to determine the morphological requirements for *1D nanowires* under which a SIT can occur.

In this Rapid Communication, we present a comparative study of homogeneous and inhomogeneous nanotube-templated wires and find a qualitatively different behavior at low temperatures. Homogeneous samples (of length $\sim$100 nm) show a SIT which occurs when the wire's normal resistance is close to R_Q, confirming previous results where different nanotubes were utilized as substrates.[2] Inhomogeneous wires, on the other hand, exhibit a mixed behavior displaying properties of superconductors and insulators at once. Such samples frequently show multiple steps in the resistive transitions but no resistive tails typical of QPS.[3–5] We propose a qualitative model which regards the inhomogeneous wire as a sequence of weak link constrictions (WLC's) connected in series. Each WLC has a certain dissipative size and corresponding normal resistance, depending on which the WLC can be either superconducting or insulating. Homogeneous (and short enough) wires do not show such mixed behavior because each wire acts as a single WLC.

The wires were fabricated using a molecular templating technique,[2] in which a single-walled carbon nanotube was suspended over a $\sim$100 nm wide trench etched into a multilayered $Si/SiO_2/SiN$ substrate. Unlike previous studies,[2,4] here we use *fluorinated* single-wall nanotubes (FSWNT), which are known to be insulating.[12] The substrate with suspended nanotubes was then sputter-coated[13] in one of the two ways: (i) with amorphous[14] $Mo_{0.79}Ge_{0.21}$ or (ii) with a slightly thinner amorphous $Mo_{0.79}Ge_{0.21}$ film followed (in the same vacuum cycle) by a 2 nm Si film. Contact pads were defined using photolithography, followed by (i) wet etching in H_2O_2 for MoGe or (ii) reactive ion etching followed by wet H_2O_2 etching for Si-coated samples. While both processes produce samples with the same geometry [Fig. 1(a)] and similar dimensions (Table I), these two fabrication meth-

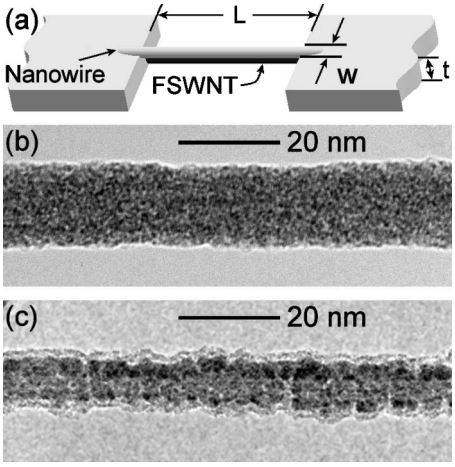

FIG. 1. (a) Sample configuration. The sample consists of two coplanar films seamlessly connected by a thin wire. (b) A TEM micrograph of a typical uncoated wire formed on a nanotube template. The MoGe thickness is 8 nm. (c) A TEM micrograph of a Si-coated MoGe wire. Sputtered MoGe thickness is 4.5 nm and Si thickness is 2 nm.

 ©2004 The American Physical Society

TABLE I. Parameters of nanowires. Samples A1–A12 are bare MoGe wires and B1–B7 are Si-coated wires. The normal resistance of nanowires (R_N) was determined from $R(T)$ curves, as indicated by an arrow for sample A1 in Fig. 3(a). Wire lengths (L) and widths (w) were measured with a SEM. Here t is the sputtered thickness of MoGe.

	R_N (k Ω)	L (nm)	w (nm)	t (nm)		R_N (k Ω)	L (nm)	w (nm)	t (nm)
A1	2.39	99	21.4	8.5	B1	4.85	126	15.4	6.0
A2	3.14	127	18.7	8.5	B2	8.30	121	14.9	4.5
A3	3.59	93	16.8	8.5	B3	9.52	139	12.1	4.5
A4	3.86	156	18.5	7.0	B4	15.26	121	11.4	3.5
A5	4.29	188	20.8	7.0	B5	16.31	123	13.8	4.0
A6	4.73	109	12.6	7.0	B6	19.30	145	15.9	4.0
A7	5.61	116	11.6	7.0	B7	44.83	115	13.0	2.0
A8	6.09	125	14.2	7.0					
A9	8.22	105	10.6	5.5					
A10	8.67	121	8.8	5.5					
A11	9.67	140	10.8	5.5					
A12	26.17	86	13.6	7.5					

ods result in different wire morphologies as revealed by transmission electron microscopy (TEM) imaging and confirmed by transport measurements (see below). The first process results in homogeneous nanowires [Fig. 1(b)], which we will refer to as "bare" wires. The second method yields inhomogeneous wires, which will be called "Si-coated" wires [Fig. 1(c)]. Although these two fabrication methods give qualitatively different wires, the exact mechanism of this is not clear. The most probable explanation is that Si introduces some surface tension that leads to the creation of grains. On the other hand, if exposed to air, the outer layer of MoGe wires oxidizes unless coated by a protective film, in our case Si. To ensure that the conducting cores of bare wires have similar dimensions as the cores of the Si-coated wires, the bare wires must be made thicker to compensate for the expected surface oxidation. Since thicker wires are typically more homogeneous than the very thin ones, our bare wires exhibit a much higher degree of homogeneity.

The oxidized layer thickness (in bare wires) can be estimated as follows (Fig. 2). For each sample, the wire length L divided by the normal state resistance R_N is plotted versus scanning electron microscopy (SEM) measured width w in Fig. 2(a). The bare wire data (circles) can be well approximated by a linear fit (dashed line), providing evidence for their homogeneous structure. The fitting parameters give an oxidized layer thickness ≈ 2.3 nm (half of the fit's x-axis intercept value) and the resistivity for MoGe $\rho \approx 180\ \mu\Omega$ cm (obtained from the fit's slope and the wire's average thickness, $d_{ave} \approx 4.7$ nm, estimated under the assumption that the top 2.3 nm of the sputtered MoGe is oxidized), in agreement with published values.[2,14] No reasonable linear fit could be obtained for the Si-coated wires (crosses), further indicating their inhomogeneous structure. In Fig. 2(b) we compare the T_c's of bare MoGe films and Si-coated MoGe films (circles and crosses, respectively) plotted versus their thicknesses. By shifting the data for bare films by 2.7 nm to the left the two families of data points overlap [Fig. 2(b)]. It is therefore concluded that the oxidized layer thickness is 2.7 nm, similar to the above estimate.

Voltage versus current measurements, $V(I)$, were performed by current biasing the sample through a large (~ 1 MΩ) resistor. Zero-bias resistance $R(T)$ was obtained from the slope of the linear part of the $V(I)$ curves as temperature was varied. Similar to Ref. 16, transport measurements were performed in ^{4}He or ^{3}He cryostats equipped with rf-filtered leads. The differential resistance vs bias current, $dV(I)/dI$, was measured using an ac excitation on top of a dc current offset generated by a low-distortion function generator (SRS-DS360).

Zero-bias resistance versus temperature measurements are compared for homogeneous [Figs. 3(a) and 3(b)] and inhomogeneous [Figs. 3(c) and 3(d)] nanowires. First note that the rightmost superconducting transition observed on *all* samples is due to the electrodes (i.e., thin MoGe films connected to the ends of the wire). Below the temperature of this transition ($T_{c,film}$) only the wire contributes to the measured

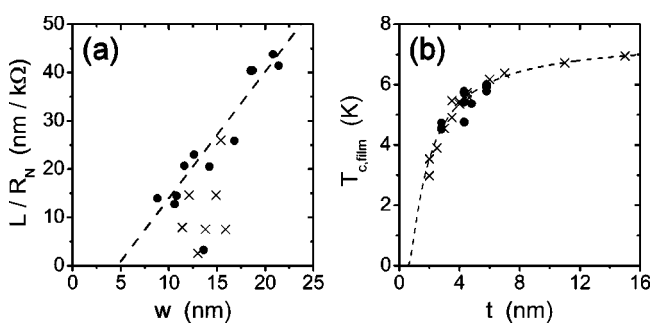

FIG. 2. (a) L/R_N vs w for bare (circles) and Si-coated (crosses) wire samples. The dashed line is a linear fit to the bare wire data, $L/R_N = (2.6\ \text{mS})(w - 4.6\ \text{nm})$. (b) Film T_c vs t for bare (circles) and Si-coated (crosses) film samples. In order for the data to agree, the bare MoGe film data have been shifted from their actual position to the left by 2.7 nm, which accounts for the thickness of the oxidized surface layer. The dashed curve is a theoretical fit [Eq. (3) in Ref. 15].

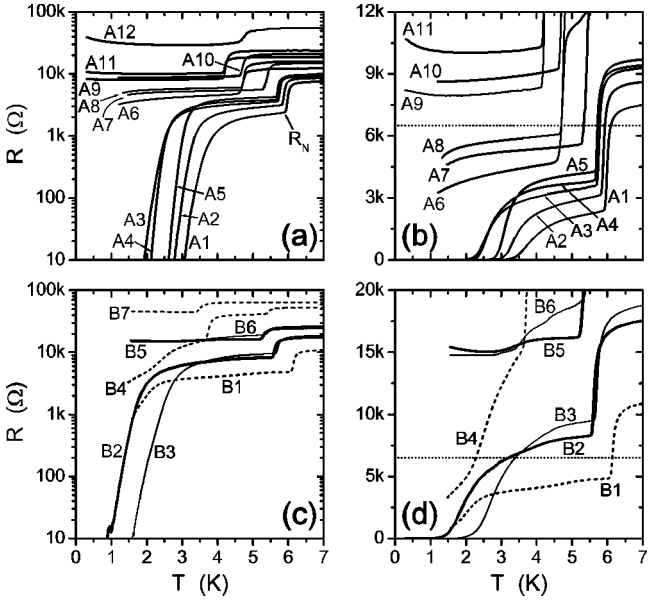

FIG. 3. Resistance vs temperature curves are shown for bare wires, which are homogeneous (a and b), and Si-coated wires, which are inhomogeneous (c and d). Figures (b) and (d) show the data on a linear scale for clarity. The horizontal dotted lines indicate the R_Q level at which the SIT occurs in homogeneous samples.

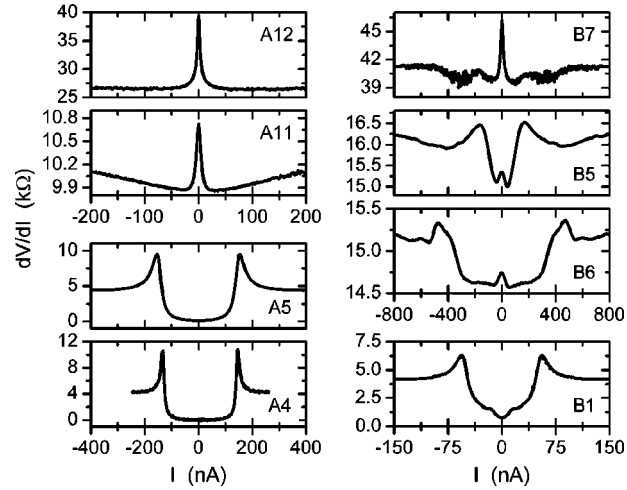

FIG. 4. Differential resistance as a function of bias current for various bare (left column) and Si-coated (right column) samples. Measurement temperatures are 0.3 K for samples A11 and A12, 2.8 K for sample A5, 2.2 K for sample A4, and 1.5 K for samples B1, B5, B6, and B7.

resistance. Therefore, in what follows we will only be interested in temperatures $T<T_{c,film}$. We first discuss the family of $R(T)$ curves for bare wire samples, presented in Fig. 3(a), which show a clear dichotomy. In the log-linear representation, samples A1–A8 all have negative curvature $[d^2\log(R)/dT^2<0]$ with more than half of these samples reaching immeasurably low resistances. Therefore, we refer to these samples as superconducting. Although samples A6, A7, and A8 do not reach such low resistances, their negative curvature as well as their decreasing resistance with decreasing temperature [Fig. 3(b)] lead us to believe they too are superconducting. Due to their smaller widths we assume that their critical temperatures are suppressed[15] such that they do not go through their full superconducting transition within the temperature range studied. Samples A9–A12 show only the transition of the film electrodes. Their curvature is always positive (for $T<T_{c,film}$) with increasing resistances as temperature is decreased. Consequently we consider these samples to be insulating. The insulating regime can be either due to a suppression of T_c to zero[15] or due to a proliferation of QPS (Ref. 17) (or both). Observation of these two regimes indicates that a superconductor-insulator transition occurs in this family of nanowires, confirming previous results.[2] This transition occurs when the wire's $R_N \approx R_Q$ [Fig. 3(b)]. Therefore it can be suggested that the R_N of the wire is the parameter that controls the SIT. However, since wire length was not varied over a wider range we cannot exclude the possibility that the cross-sectional area of the wire is the control parameter.

Measurements presented in Fig. 3 demonstrate that bare and Si-coated wires are qualitatively different. In the Si-coated wires the $R(T)$ curves are less predictable, show multiple steps or "humps" [Figs. 3(c) and 3(d)], and in some cases exhibit a mixed behavior that does not always allow them to be clearly identified as either superconducting or insulating. For example, sample B4 shows three steps on the $R(T)$ curve and a tail at the lowest temperature, which could be the beginning of the fourth transition. The first step, as always, reflects the superconducting transition in the electrodes, but the other steps correspond to some weak links in the wire itself. Some Si-coated wires exhibit both positive and negative curvature at different temperatures. Such mixed behavior is seen in samples B5 and B6, with their resistance initially dropping as in superconducting wires (i.e., with a negative curvature) but then starting to increase as in insulating wires. The conclusion is that no clear SIT at $R_N \approx R_Q$ can be observed in the family of nonhomogeneous wires.

A clear difference between bare and Si-coated wires is also found in the $dV(I)/dI$ measurements (Fig. 4). Bare MoGe wires (left column) again show one of only two distinct types of behavior. The superconducting wires exhibit a large minimum centered around zero bias (e.g., A4 and A5) and peaks at the bias current which is equal to the critical current of the nanowire. The insulating samples show a single zero-bias resistance peak (e.g., A11 and A12). This is in agreement with previous experiments.[2]

The Si-coated MoGe wires, on the other hand, frequently show various combinations of such types of behavior. For example, sample B5 has a clear resistance depression in the range ± 150 nA with the critical current peaks at the limits of this depression, and, in addition to this, a narrow zero-bias resistance peak. Such mixed behavior indicates that some parts of the wire are superconducting while other sections appear insulating. Sample B6 also shows similar results. This fact again confirms that these wires are not homogeneous.

The properties of inhomogeneous wires can be understood by assuming that they contain a sequence of independent weak link constrictions, each surrounded by a dissipative region, the size of which determines the normal resistance of the WLC. Since the free-energy barriers for

phase slips are different in each such WLC and the constrictions are connected in series it is clear that $R(T)$ curves should show crossings[5] and multiple steps [such as for sample B4 in Fig. 3(c)]. Moreover some links can be insulating if their normal resistance is large enough, similar to homogeneous wires. For example, sample B5 shows a mixed behavior that is explained by assuming it contains two WLC's—one superconducting and one insulating. The $R(T)$ curve then should show one superconducting hump and a tail with increasing resistance at lower temperatures, typical of insulating wires. Likewise, a single superconducting feature and an insulating zero-bias peak should be observed in the $dV(I)/dI$ curve. These characteristics are indeed observed [Figs. 3(d) and 4]. In some wires all WLC's can be superconducting, as for example, in sample B1 (and possibly B2, B3, and B4). In the case of B1, two humps in the $R(T)$ curve (at $T\approx 5$ K and $T\approx 2$ K) and two superconducting peaks on $dV(I)/dI$, corresponding to two critical currents (at $I\approx 15$ nA and $I\approx 60$ nA), are observed, indicating that two superconducting WLCs are present. Finally, since each insulating WLC produces a single $dV(I)/dI$ peak located at zero current, the wires with a few insulating WLC's should nevertheless exhibit only one peak at zero bias, as could be the case for sample B7 in Fig. 4.

All measured homogeneous samples act as superconductors if they satisfy $R_N < R_Q$ and as insulators otherwise [Fig. 3(b)]. Inhomogeneous wires frequently violate this condition, as for example sample B2 [Fig. 3(d)]. This can be explained by the WLC model and by assuming that each WLC can be either insulating or superconducting depending on its own normal resistance. The sample B2 has shown two distinguishable peaks on its $dV(I)/dI$ curve (not shown), corresponding to two superconducting WLC's with slightly different critical currents. Since this sample's normal resistance is 8.30 kΩ and since two similar WLC's are detected in this wire, it can be estimated that the normal resistance of each WLC is ≈ 4.15 kΩ. Thus each WLC is superconducting and hence the entire wire is superconducting as well.

Since each WLC is manifest by a jumpwise increase of the sample resistance at the WLC's critical current, it is reasonable to associate WLC's with phase slip centers[18,19] (which are usually positioned at weak spots along the wire). The normal resistance of a WLC is then the resistance of the dissipative region or the region which is populated by quasiparticles generated by the phase slip center. This dimension is the quasiparticle diffusion length, $\Lambda_Q \approx (D\tau_E)^{1/2} \approx 100$ nm, where $D\approx 10^{-4}$ m^{2}s is the diffusion constant and $\tau_E \approx 10^{-10}$ s is the inelastic scattering time.[18–20] If constrictions are present in the wire, Λ_Q is further reduced and equals the distance between the constrictions. Our short homogeneous wires are not longer than Λ_Q, so each wire acts as a single WLC. These wires therefore show a clear SIT. Inhomogeneous wires have more than one WLC (i.e., will develop more than one phase slip center under strong current bias) and consequently show a mixed behavior.

In summary, we have found that the morphology of superconducting nanowires has a strong effect on the observed superconductor-insulator transition. A clear SIT is only found in homogeneous wires whereas inhomogeneous samples show a smeared transition and mixed behavior. In the latter case, the results are understood by the assumption that inhomogeneous wires are composed of weakly coupled sections connected in series. Each section exhibits either superconducting or insulating behavior while the entire wire shows a mixed behavior. Further understanding of the SIT will require a study of wires with a wider length variation. Such work is currently in progress.

This work was supported by NSF CAREER Grant No. DMR 01-34770 and by the Alfred P. Sloan Foundation. Some fabrication was performed at CMM-UIUC supported in part by DOE Grant No. DEFG02-96-ER45439.

[1] P. Xiong, A.V. Herzog, and R.C. Dynes, Phys. Rev. Lett. **78**, 927 (1997).
[2] A. Bezryadin, C.N. Lau, and M. Tinkham, Nature (London) **404**, 971 (1999).
[3] N. Giordano, Phys. Rev. Lett. **61**, 2137 (1988).
[4] C.N. Lau, N. Markovic, M. Bockrath, A. Bezryadin, and M. Tinkham, Phys. Rev. Lett. **87**, 217003 (2001).
[5] C.N. Lau, Ph.D. thesis, Harvard University, 2001.
[6] A. Frydman, Physica C **391**, 189 (2003).
[7] J.M. Valles, Jr., Shih-Ying Hsu, R.C. Dynes, and J.P. Garno, Physica B **197**, 522 (1994).
[8] A.M. Finkel'stein, Physica B **197**, 636 (1994).
[9] D.B. Haviland, Y. Liu, and A.M. Goldman, Phys. Rev. Lett. **62**, 2180 (1989); A. Goldman and N. Markovic, Phys. Today **51** (11), 39 (1998).
[10] R.P. Barber, Jr., L.M. Merchant, A. La Porta, and R.C. Dynes, Phys. Rev. B **49**, 3409 (1994).
[11] A. Frydman, O. Naaman, and R.C. Dynes, Phys. Rev. B **66**, 052509 (2002).
[12] E.T. Mickelson *et al.*, Chem. Phys. Lett. **296**, 188 (1998).
[13] The sputtering was DC for MoGe and RF for the Si overlayer. The sputterer was equipped with an LN_2 cold trap.
[14] J.M. Graybeal and M.R. Beasley, Phys. Rev. B **29**, 4167 (1984).
[15] Y. Oreg and A.M. Finkel'stein, Phys. Rev. Lett. **83**, 191 (1999).
[16] A. Rogachev and A. Bezryadin, Appl. Phys. Lett. **83**, 512 (2003).
[17] A.D. Zaikin, D.S. Golubev, A. van Otterlo, and G.T. Zimanyi, Phys. Rev. Lett. **78**, 1552 (1997).
[18] W.J. Skocpol, M.R. Beasley, and M. Tinkham, J. Low Temp. Phys. **16**, 145 (1974).
[19] R. Tidecks, *Current-Induced Nonequilibrium Phenomena in Quasi-One-Dimensional Superconductors* (Springer-Verlag, New York, 1990).
[20] J.M. Graybeal, Ph.D. thesis, Stanford University, 1985.